

Enhancing classification accuracy through chaos

Panos Stinis

*Advanced Computing, Mathematics and Data Division, Pacific Northwest
National Laboratory, Richland WA 99354*

Abstract

We propose a novel approach which exploits chaos to enhance classification accuracy. Specifically, the available data that need to be classified are treated as vectors that are first lifted into a higher-dimensional space and then used as initial conditions for the evolution of a chaotic dynamical system for a prescribed temporal interval. The evolved state of the dynamical system is then fed to a trainable softmax classifier which outputs the probabilities of the various classes. As proof-of-concept, we use samples of randomly perturbed orthogonal vectors of moderate dimension (2 to 20), with a corresponding number of classes equal to the vector dimension, and show how our approach can both significantly accelerate the training process and improve the classification accuracy compared to a standard softmax classifier which operates on the original vectors, as well as a softmax classifier which only lifts the vectors to a higher-dimensional space without evolving them. We also provide an explanation for the improved performance of the chaos-enhanced classifier.

Introduction

Classification is one of the two fundamental supervised machine learning (ML) tasks [1, 2], the other being regression [3, 4]. It is a vast research topic with applications ranging from health [5] to finance [6] to science [7, 8, 9]. The objective of ML-based classification is to train a ML tool to assign the correct class (label) to each member of a dataset. Usually, ML-based classifiers assign, for each member of a dataset, a probability for the member to belong to each of the available classes.

Due to the pervasive nature of classification, there are many algorithms that have been developed for this task and an exhaustive comparison is

beyond the scope of the current work. Instead, we will reduce the ML-classification problem to its bare essentials and offer a novel approach which can both accelerate training and improve the training/testing accuracy. The approach we will discuss can be applied directly to the raw input data or to the latent space representation of the data provided by an existing algorithm (before the final linear output layer which connects to a softmax classifier that assigns probabilities to the various classes).

Specifically, we consider a dataset consisting of randomly perturbed orthogonal vectors of a prescribed dimension. The correct class for each of the perturbed orthogonal vectors is the direction corresponding to the unperturbed vector. The baseline model we will use consists of a trainable softmax classifier to which we feed the randomly perturbed orthogonal vectors. The novel approach we propose consists of two stages: (i) lifting the vector to a higher dimension, and (ii) identifying the lifted vector as the initial state of a chaotic dynamical system and evolving it for a prescribed temporal interval before it is processed by the trainable softmax classifier. Our purpose in this work is to disentangle the effect that the two stages can have on the classification training time and accuracy, so that the observed improvement over the baseline model, which can be significant, can be explained.

Section 1 presents the various constructions including the baseline classifier model, the lifting to higher dimensions and the chaos-enhanced model. Section 2 contains numerical results for the various constructions along with an explanation of the improved performance of the chaos-enhanced classifier, while Section 3 offers a discussion of the proposed approach and directions for future work.

1 Chaos-enhanced classification

Consider a collection $V_N = [v_1, v_2, \dots, v_N]$ of N vectors of dimension m , each being a random perturbation of a canonical basis vector in \mathbb{R}^m . The canonical basis in m dimensions consists of the vectors $e_i = [0, \dots, 0, 1, 0, \dots, 0]^T$,

for $i = 1, \dots, m$, with all 0s except for the 1 at the i -th coordinate. For symmetry, we will assume that the m canonical basis vectors are equally represented in the collection, say with N_{class} vectors each, so $N = m \times N_{class}$. Each of the N vectors is formed by adding samples from independent, normally distributed random variables with mean zero and prescribed variance to all the coordinates. Thus, each of the N vectors in V_N can be written as $v_{nk} = e_{i_{nk}} + \epsilon_{nk}$, for $n = 1, \dots, N$ and $k = 1, \dots, m$, where $\epsilon_{nk} \sim \mathcal{N}(0, \sigma)$

with σ prescribed and i_n is the index corresponding to the canonical vector that we use to build the n -th sample in the collection.

Baseline model. The baseline model consists of a trainable softmax classifier to which each of the N vectors are fed. Since we consider the N vectors coming from random perturbations of the canonical basis vectors in \mathbb{R}^m , we consider m classes, one for each of the m orthogonal directions in \mathbb{R}^m . As a result, the trainable weights of the linear output layer of the softmax classifier are the elements of a $m \times m$ matrix W , denoted by w_{ij} for $i, j = 1, \dots, m$. For a vector v_n from the collection of N vectors, the softmax classifier takes as input the logits $z_{ni} = \sum_{j=1}^m W_{ij}v_{nj}$ for $i = 1, \dots, m$, and outputs the m probabilities

$$p_{ni} = \frac{e^{z_{ni}}}{\sum_{i=1}^m e^{z_{ni}}}, \text{ for } i = 1, \dots, m, \quad (1)$$

that the vector v_n belongs to each of the m classes. We employ cross-entropy as the loss function to train the elements of W and use the Adam optimizer for training. The cross-entropy loss for the N vectors is defined as

$$L_N = -\frac{1}{N} \sum_{n=1}^N \sum_{l=1}^m \chi_{nl} \log p_{nl}, \quad (2)$$

where $\chi_{nl} = 1$ if $l = i_n$ and 0 otherwise, where i_n is the true class of the n -th sample, and p_{nl} is provided by (1). The derivative of the cross-entropy loss function with respect to an element of the weight matrix W is given by

$$\frac{\partial L_N}{\partial w_{ij}} = -\frac{1}{N} \sum_{n=1}^N [\chi_{ni} - p_{ni}] v_{nj}, \text{ for } i, j = 1, \dots, m. \quad (3)$$

Since the true classes of the vectors in V_N are along the directions of the canonical basis vectors in \mathbb{R}^m , the training of the baseline model aims to suppress the random perturbations along the m directions (as can be seen by (3)).

Algorithm 1 Baseline classification algorithm

Input: Number of classes m , data V_N (vectors of dimension m) where $N = m \times N_{class}$ (N_{class} orthogonal vectors from each of the m classes perturbed with $\mathcal{N}(0, \sigma)$ noise, σ is user-prescribed), number of training data N_{train} and test data N_{test} with $N_{train} + N_{test} = N$, class labels χ for the vectors in V_N , mini-batch size N_b , initial learning rate for Adam optimizer η , number of training epochs N_{epochs}

- 1: **Training:**
 - 2: Initialization of the $m \times m$ weight matrix W
 - 3: **for** each training epoch $n = 1, 2, \dots, N_{epochs}$ **do**
 - 4: Pick a mini-batch from the training data $V_{N_{train}}$
 - 5: Assign class probabilities to the mini-batch using a softmax classifier
 - 6: Use the Adam optimizer with cross-entropy loss function to update the weight matrix W
 - 7: Repeat until the epoch is completed
 - 8: **end for**
-

Lifting-enhanced model. As we have already discussed, the proposed approach can be divided into two stages: (i) lifting each of the N vectors to a higher dimension and (ii) evolving the lifted vector using a chaotic dynamical system. The first stage can be considered in isolation from the second one, since it can be beneficial for classification to lift, within reason, the dimensionality of the vectors to be classified [10, 11, 12]. There are various methods to lift a vector to higher dimensions, e.g., zero-padding, polynomial feature mapping, tensor product. Each of the N vectors of dimension m is lifted to a vector of dimension m_{lift} . As a result of the lifting process, the linear output layer weight matrix W^{lift} has dimensions $m \times m_{lift}$. For the n -th original (unlifted) vector $v_n = [v_{n1}, \dots, v_{nm}]^T$, the corresponding lifted vector, denoted by v_n^{lift} , is defined as

$$v_n^{lift} = [\eta_1, \eta_2, \eta_3, v_{n1}, \dots, v_{nm}, \eta_4, \dots, \eta_{m_{lift}-m}]^T, \quad (4)$$

where $\eta_1, \dots, \eta_{m_{lift}-m}$ are random linear combinations of the m coordinates. Specifically, $\eta_j = \sum_{l=1}^m \epsilon_l v_{nl}$ where $\epsilon_l \sim \mathcal{N}(0, \frac{1}{m_{lift}})$. The specific choice of the lifting construction is due to the structure of the Lorenz 96 model that is used to evolve the lifted vector, namely the need to enforce periodicity (see (10) below). If the constraints from the Lorenz 96 system were not there, we could have picked a simpler lifting construction e.g.,

$$v_n^{lift} = [v_{n1}, \dots, v_{nm}, \eta_1, \dots, \eta_{m_{lift}-m}]^T. \quad (5)$$

We note that the chosen lifting approach is not optimized, but does imbue the added coordinates with randomly distorted information from the m coordinates of the original vector. Also, the lifting of each vector to one which preserves the m coordinates of the original vector but adds (small) random perturbations in the remaining coordinates can be understood as a random regularization mechanism. This is because the weight matrix W^{lift} will be trained to map from $\mathbb{R}^{m_{lift}}$ to the m classes, thus it will be trained to suppress random perturbations in the $m_{lift}-m$ dimensions (in addition to learning to suppress random perturbations in the m coordinates like the baseline model). Improving training accuracy through adding random perturbations to data is a well-known practice for neural networks [13, 14, 15, 16]. When we present the numerical results (Section 2), we provide a more quantitative explanation as to how the lifting to a higher dimensional space aids the classification task.

Due to the lifting of the vectors to m_{lift} dimensions, the logits $z_{ni}^{lift} = \sum_{j=1}^{m_{lift}} W_{ij}^{lift} v_{nj}^{lift}$ for $i = 1, \dots, m$, and softmax outputs the m probabilities

$$p_{ni}^{lift} = \frac{e^{z_{ni}^{lift}}}{\sum_{i=1}^m e^{z_{ni}^{lift}}}, \quad \text{for } i = 1, \dots, m, \quad (6)$$

that the vector v_n^{lift} belongs to each of the m classes. The loss function is given by

$$L_N^{lift} = -\frac{1}{N} \sum_{n=1}^N \sum_{l=1}^m \chi_{nl}^{lift} \log p_{nl}^{lift}, \quad (7)$$

where $\chi_{nl}^{lift} = \chi_{nl}$ i.e., the class of each lifted vector remains the same, and p_{nl}^{lift} is provided by (6). The derivative of the cross-entropy loss function L_N^{lift} with respect to an element of the weight matrix W^{lift} is given by

$$\frac{\partial L_N^{lift}}{\partial w_{ij}^{lift}} = -\frac{1}{N} \sum_{n=1}^N [\chi_{ni}^{lift} - p_{ni}^{lift}] v_{nj}^{lift}, \quad \text{for } i = 1, \dots, m \text{ and } j = 1, \dots, m_{lift}. \quad (8)$$

Algorithm 2 Lifting-enhanced classification algorithm

Input: Number of classes m , data V_N (vectors of dimension m) where $N = m \times N_{class}$ (N_{class} orthogonal vectors from each of the m classes perturbed with $\mathcal{N}(0, \sigma)$ noise, σ is user-prescribed), number of training data N_{train} and test data N_{test} with $N_{train} + N_{test} = N$, class labels χ for the vectors in V_N , lifting dimension m_{lift} ($m_{lift} > m$), mini-batch size N_b , initial learning rate for Adam optimizer η , number of training epochs N_{epochs}

- 1: **Lifting:**
 - 2: Create the m_{lift} -dimensional lifted data V_N^{lift} using (4)
 - 3: **Training:**
 - 4: Initialization of the $m \times m_{lift}$ weight matrix W^{lift}
 - 5: **for** each training epoch $n = 1, 2, \dots, N_{epochs}$ **do**
 - 6: Pick a mini-batch from the training data $V_{N_{train}}^{lift}$
 - 7: Assign class probabilities to the mini-batch using a softmax classifier
 - 8: Use the Adam optimizer with cross-entropy loss function to update the weight matrix W^{lift}
 - 9: Repeat until the epoch is completed
 - 10: **end for**
-

Chaos-enhanced model. While lifting to higher dimensions can improve classification accuracy, even more significant improvement can be achieved if we further employ chaos. Specifically, each lifted vector, which is a point in an m_{lift} -dimensional space, can be identified as the initial state of a chaotic dynamical system and evolved for a prescribed temporal interval. The obvious question is why should such a process aid the classification accuracy? Intuitively, a chaotic dynamical system increases the distance of states that are initially close. In our case, the vectors resulting from the lifting process already contain randomness in the $m_{lift} - m$ dimensions. However, a controlled evolution under a chaotic dynamical system can pull those vectors apart, in essence homogenizing the randomness in all m dimensions. This results in a more efficient use of the high dimensionality of the lifting space (this statement will become more concrete quantitatively in Section 2).

For our numerical experiments we have employed the Lorenz 96 model [17]. The model is defined as

$$\frac{dx_i}{dt} = (x_{i+1} - x_{i-2})x_{i-1} - x_i + F, \quad \text{for } i = 1, \dots, K, \quad (9)$$

$$\text{with } x_{-1} = x_{K-1}, \quad x_0 = x_K, \quad x_{K+1} = x_1, \quad K \geq 4, \quad (10)$$

and F is a forcing term. Based on the literature, we have chosen the value $F = 8$ for all the numerical experiments, although a more detailed study of the effect of F on the results will be interesting [18]. Also, because of the lower bound on K from (9), the 3 periodicity conditions in (10) and the lifting construction, in our numerical experiments we consider lifting spaces of dimension $m_{lift} \geq m + 6$.

An important question to ask is about the length of the temporal interval T for which one should evolve the chaotic dynamical system so that it is beneficial for the classification accuracy [19]. Based on dynamical system theory, a Lyapunov time is the time it takes for the deviation between two initial conditions to grow by a factor of e . Thus, a few Lyapunov times is a good indicator of a chaotic system's predictability. Based on Lyapunov time estimates for the Lorenz 96 model (around 0.6 units of time for the regimes studied in the literature [18, 20]), we chose $T = 2$ units of time for our numerical experiments (except where noted).

We denote the n -th lifted and chaos-evolved data vector as $v_n^{lift,chaos}$. As a result, the logits $z_{ni}^{lift,chaos} = \sum_{j=1}^{m_{lift}} W_{ij}^{lift} v_{nj}^{lift,chaos}$ for $i = 1, \dots, m$, and softmax outputs the m probabilities

$$p_{ni}^{lift,chaos} = \frac{e^{z_{ni}^{lift,chaos}}}{\sum_{i=1}^m e^{z_{ni}^{lift,chaos}}}, \quad \text{for } i = 1, \dots, m, \quad (11)$$

that the vector $v_n^{lift,chaos}$ belongs to each of the m classes. The loss function is given by

$$L_N^{lift,chaos} = -\frac{1}{N} \sum_{n=1}^N \sum_{l=1}^m \chi_{nl}^{lift,chaos} \log p_{nl}^{lift,chaos}, \quad (12)$$

where $\chi_{nl}^{lift,chaos} = \chi_{nl}$ i.e., the class of each lifted and chaos-evolved vector remains the same, and $p_{nl}^{lift,chaos}$ is provided by (11). The derivative of the cross-entropy loss function $L_N^{lift,chaos}$ with respect to an element of the weight matrix $W^{lift,chaos}$ is given by

$$\frac{\partial L_N^{lift,chaos}}{\partial w_{ij}^{lift,chaos}} = -\frac{1}{N} \sum_{n=1}^N [\chi_{ni}^{lift,chaos} - p_{ni}^{lift,chaos}] v_{nj}^{lift,chaos}, \quad (13)$$

for $i = 1, \dots, m$ and $j = 1, \dots, m_{lift}$.

Algorithm 3 Lifting- and chaos-enhanced classification algorithm

Input: Number of classes m , data V_N (vectors of dimension m) where $N = m \times N_{class}$ (N_{class} orthogonal vectors from each of the m classes perturbed with $\mathcal{N}(0, \sigma)$ noise, σ is user-prescribed), number of training data N_{train} and test data N_{test} with $N_{train} + N_{test} = N$, class labels χ for the vectors in V_N , lifting dimension m_{lift} ($m_{lift} \geq 7$), dimension of Lorenz 96 model K ($K = m_{lift} - 3$), forcing magnitude F , temporal interval for chaotic evolution T , timestep for chaotic evolution η_{chaos} , mini-batch size N_b , initial learning rate for Adam optimizer η , number of training epochs N_{epochs}

- 1: **Lifting:**
 - 2: Create the m_{lift} -dimensional lifted data V_N^{lift} using (4)
 - 3: **Chaotic evolution:**
 - 4: Identify each datapoint in V_N^{lift} as an initial condition for Lorenz 96 and evolve for T units of time with timestep η_{chaos} using (9)-(10) to create the data $V_N^{lift,chaos}$
 - 5: **Training:**
 - 6: Initialization of the $m \times m_{lift}$ weight matrix $W^{lift,chaos}$
 - 7: **for** each training epoch $n = 1, 2, \dots, N_{epochs}$ **do**
 - 8: Pick a mini-batch from the training data $V_{N_{train}}^{lift,chaos}$
 - 9: Assign class probabilities to the mini-batch using a softmax classifier
 - 10: Use the Adam optimizer with cross-entropy loss function to update the weight matrix $W^{lift,chaos}$
 - 11: Repeat until the epoch is completed
 - 12: **end for**
-

2 Results

2.1 Numerical experiments setup

We have conducted numerical experiments to compare the baseline model, the lifting-enhanced model, and the lifting- and chaos-enhanced model for moderate number of dimensions (classes) $m = 2, \dots, 20$. Because we want to have an equal number of samples from each class, the total number of samples varies for the different values of m . We chose $N_{class} = 20$ samples from each class, so the number of samples for each value of m is equal to $20 \times m$. The variance of the random perturbations of the orthogonal vectors was set to $\sigma = 10^{-4}$ for all the experiments. Also, we split the samples equally between those used for training and those used for testing. For

the Adam optimizer, we set the mini-batch size to $N_b = 10$ and learning rate $\eta = 10^{-3}$. We have added to the loss function of the baseline model, the lifting-enhanced model and the lifting- and chaos-enhanced model the square of the L_2 norm of the weight matrix elements multiplied by 10^{-3} as a regularizer to the cross-entropy loss. The Lorenz 96 model was evolved with the standard 4th order Runge-Kutta scheme and $\eta_{chaos} = 10^{-2}$. All the calculations were performed in double precision.

Since we do not have yet a good way to decide on the optimal value of the lifting dimension, we conducted experiments where for each value of m , we searched for the optimal lifting dimension m_{lift} between the values $m + 6$ and 50. The optimal value of m_{lift} was decided based on an accuracy metric evaluated on the *test* data. We chose the value of m_{lift} that resulted in the highest test accuracy during training. In our experiments, the optimal value of m_{lift} fluctuated due to the stochasticity of the algorithm (random perturbations of the orthogonal vectors, randomness of the values of the components in the lifted dimensions and randomness of the Adam optimizer). A more detailed study of the optimal m_{lift} will be presented elsewhere.

There are different metrics for the accuracy of the predicted class probabilities. The proportion accuracy metric is given by

$$accuracy_{proportion} = \frac{1}{N} \sum_{n=1}^N \delta_{i_{max} i_n}, \quad (14)$$

where $i_{max} = \arg \max(p_{n1}, p_{n2}, \dots, p_{nm})$ is the predicted class for the n -th sample and i_n is the actual class. For the proportion accuracy metric to be 1, it is only required that the predicted class probability for the correct class is larger than the predicted class probabilities for the rest of the classes. This metric is not stringent enough to distinguish between the various models. Instead, we have opted for the following accuracy metric

$$accuracy_{alignment} = \frac{1}{N} \sum_{n=1}^N \chi_n \cdot p_n = \frac{1}{N} \sum_{n=1}^N \sum_{l=1}^m \chi_{nl} p_{nl} = \frac{1}{N} \sum_{n=1}^N p_{ni_n}, \quad (15)$$

where $\chi_{nl} = \delta_{li_n}$ (recall that i_n is the correct class for the n -th sample) and p_{nl} is the probability for class l for the n -th sample predicted by one of the 3 models we compared (we note that N in (15) stands for N_{train} or N_{test} depending on whether we measure training accuracy or testing accuracy). We see from (15) that to achieve 100% accuracy, the predicted probability from the model for the correct label for each sample must be 1. Another way

to interpret the metric in (15) is as confidence of the predicted class labels by the model, since it measures the *alignment* between the predicted class probabilities vector and the correct class vector. Unless otherwise stated, the accuracy used in the figures is the alignment accuracy metric (although we utilize the proportion metric too in Section 2.4 to discuss robustness).

2.2 Observations from results

Figures 1-3 show the evolution of the loss (cross-entropy) and the accuracy with epochs for the training and testing for the 3 models when $m = 2, 10, 20$. Recall that we chose the optimal value of m_{lift} based on the test accuracy. The results lead to various observations about the performance of the 3 models.

First, while the lifting alone can improve performance over the baseline model, there is a dramatic acceleration of the decrease rate of the loss function and an equally dramatic acceleration of the convergence of the predicted accuracy to 1 (100%) for the lifting- and chaos-enhanced model. This model can converge to perfect accuracy within a few epochs, while the corresponding loss is decreased to very small values. In fact, we had to put a lower threshold for the loss at 10^{-10} and terminate the algorithm when it was crossed, because the Adam optimizer sometime became unstable when the next epoch decreased the loss value from 10^{-10} to a value close to machine precision (10^{-16}) for our double precision calculations.

Second, the lifting- and chaos-enhanced model can reach perfect accuracy within a few hundred epochs (we allowed not more than 500 during our experiments), while the lifting-enhanced model, with the exception of $m = 2$, requires an order of magnitude more epochs to reach similar accuracy (if at all). For $m = 2$, the baseline model needs 20000 epochs to reach similar accuracy, while for $m = 10$ and $m = 20$ it is not able to do so.

Third, while the loss value decreases monotonically for the baseline and lifting-enhanced models for all values of m , for the lifting- and chaos-enhanced model for $m = 10$ and $m = 20$, the training and test loss values initially go through a phase of increase before they start decreasing. It is not accidental that during the same phase, the accuracy of the lifting- and chaos-enhanced model is lower than that of the lifting-enhanced model. This behavior is intriguing and needs to be investigated more, since the lifting- and chaos-enhanced model behaves in a way similar to some evolutionary models which perform excursions in the solution landscape before honing on an accurate one (called the steppingstone principle [21]). Of course, in the present model, there is no exploration during the optimization phase, but it

is possible that the chaotic evolution which precedes the optimization step creates an appropriate warping of the data that favors such kind of behavior.

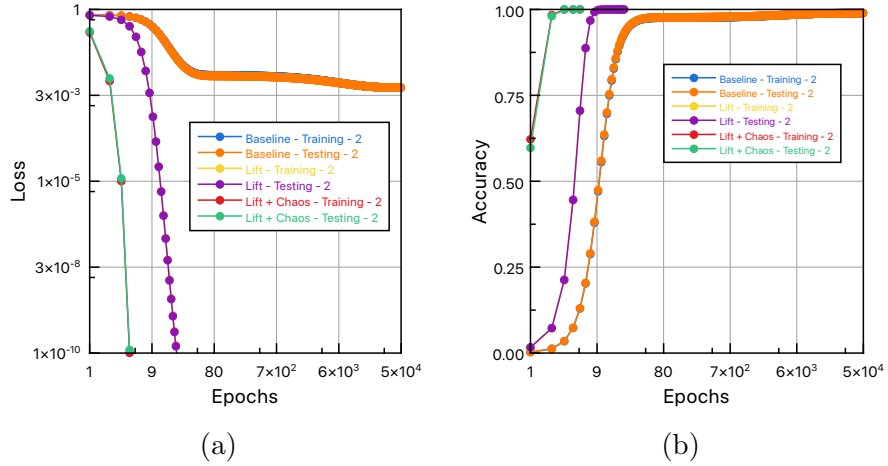


Figure 1: $m = 2$. Comparison of the baseline model, the lifting-enhanced model, and the lifting- and chaos-enhanced model (with the optimal lifting dimension). (a) Evolution of loss (cross-entropy) with epochs. (b) Evolution of accuracy with epochs.

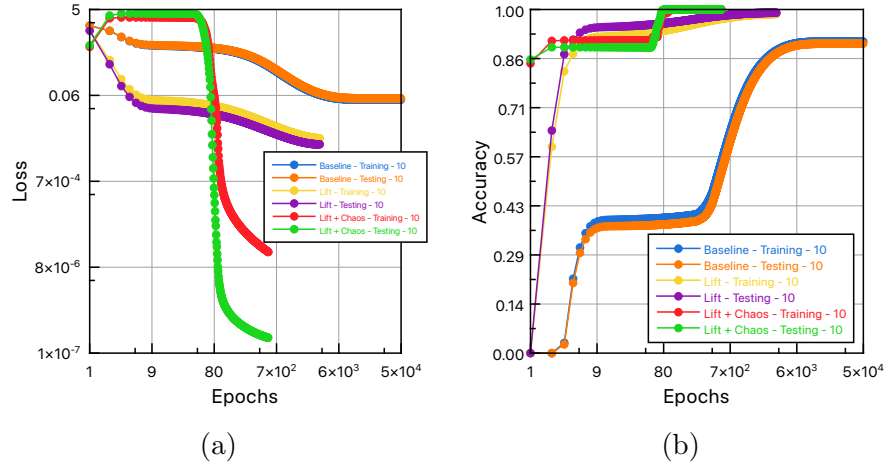


Figure 2: $m = 10$. Comparison of the baseline model, the lifting-enhanced model, and the lifting- and chaos-enhanced model (with the optimal lifting dimension). (a) Evolution of loss (cross-entropy) with epochs. (b) Evolution of accuracy with epochs.

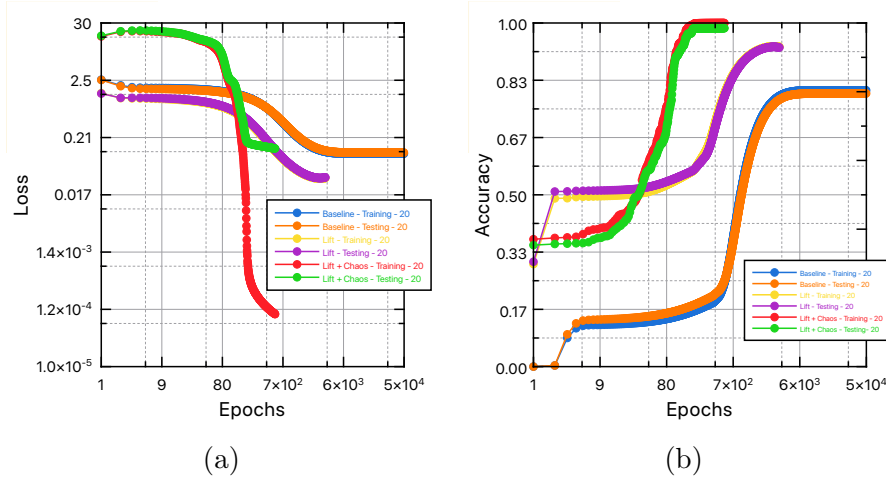


Figure 3: $m = 20$. Comparison of the baseline model, the lifting-enhanced model, and the lifting- and chaos-enhanced model (with the optimal lifting dimension). (a) Evolution of loss (cross-entropy) with epochs. (b) Evolution of accuracy with epochs.

Fourth, we observe in Fig. 3 that the test loss value for the lifting- and chaos-enhanced model is significantly larger than the training loss value, yet the test accuracy does not suffer significantly (it plateaus at 98.5%). This is likely due to an outlier which results in rather small correct class probability prediction and gets penalized logarithmically for the loss function but only linearly for the accuracy metric. The reason for the outlier could be tied to the temporal interval T of chaotic evolution being too long for some samples so their class label may be mistakenly identified if they venture into the region corresponding to a different class (see also the results below for $T = 1.5$ instead of $T = 2$ and where this phenomenon does not occur). We have included this experiment on purpose to emphasize that these results do not involve any hyperparameter optimization and this is something that we will comment on briefly now and address with a more elaborate study appearing in future work. Specifically, in all the experiments presented in Figs. 1-3, we have fixed the temporal interval of the chaotic evolution to $T = 2$ and the learning rate of the Adam optimizer is $\eta = 10^{-3}$. Both choices were based on prior experience but they were not optimized in the usual manner. To show that the results of the lifting- and chaos-enhanced model can improve even more, we will start by examining sensitivity of the accuracy to the lifting dimension m_{lift} for different values of T and η .

Figure 4 shows the evolution of training and testing accuracy with the

lifting dimension for the lifting- and chaos-enhanced model for two different values of the Adam optimizer learning rate η , namely $\eta = 10^{-3}$ and $\eta = 5 \times 10^{-4}$. We keep the maximum number of training epochs equal to 500 in both cases. We observe that while the training accuracy is equally good for the two learning rates, the testing accuracy is higher when $\eta = 5 \times 10^{-4}$.

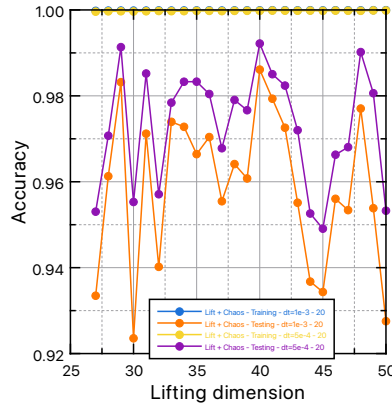


Figure 4: $m = 20$. Evolution of training and testing accuracy with the lifting dimension for the lifting- and chaos-enhanced model for two different values of the Adam optimizer learning rate η .

We continue with the examination of the effect of the chaotic evolution temporal interval value T on the accuracy for different lifting dimensions. Fig. 5(a) shows the evolution of the training and testing accuracy with lifting dimension for two values of the temporal interval, namely $T = 1.5$ and $T = 2$. We observe that $T = 1.5$ leads consistently to higher testing accuracy than $T = 2$, implying better generalization capability. Also, Fig. 5(b) shows that for $T = 1.5$, the testing loss tracks closely the training accuracy, in contrast to the results for $T = 2$.

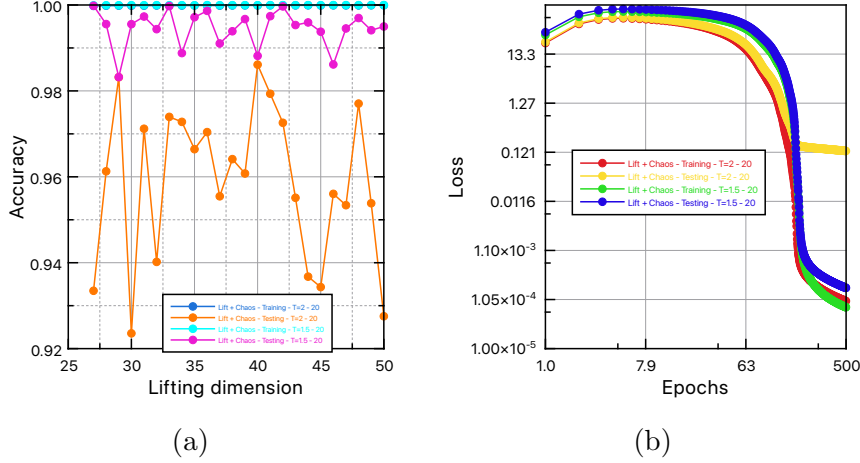


Figure 5: $m = 20$. (a) Evolution of training and testing accuracy with the lifting dimension for the lifting- and chaos-enhanced model for two different values of the chaotic evolution temporal interval T . (b) Evolution of training and testing accuracy with epochs for the optimal lifting dimension of the lifting- and chaos-enhanced model for two different values of the chaotic evolution temporal interval T .

2.3 Reason for improvement over the baseline model

The improvement in classification accuracy that is evident for the lifting-enhanced model but especially for the lifting- and chaos-enhanced model warrants an explanation. Each row of the weight matrix is a vector in m_{lift} -dimensional space and each row corresponds to 1 class. In Fig. 6 we plot the ratio of the standard deviation over the mean of the absolute value of the weight matrix row components for each row (class) for $m = 20$. This metric shows how spread are the values of the weights in each row of the weight matrix. From Fig. 6 we see that the ratio is much lower for the lifting-enhanced model and the lifting- and chaos-enhanced model than for the baseline model. This means that the components across each row of the weight matrix are much more similar for these two models than for the baseline model. Also, the ratio values are within a small range across rows (classes). A plausible explanation for this phenomenon is that the 2 models which operate in the m_{lift} -dimensional space converge through training to rows of the weight matrix (1 per class) which reside close to the corners of m_{lift} -dimensional hypercubes. In this way, the components of each row may have different signs but similar absolute value. As a result, the rows of the

weight matrix (seen as vectors) spread apart in the m_{lift} -dimensional space and facilitate classification since it is easier to be distinct from one another.

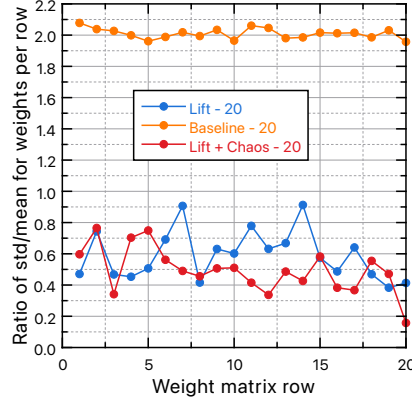


Figure 6: $m = 20$. Ratio of the standard deviation over the mean of the absolute value of the components of each row of the weight matrix for the 3 models. Note that each row of the weight matrix corresponds to a class.

We plot in Fig. 7 the value of the weights across a row of the weight matrix for different rows (recall that each row corresponds to 1 class). We plot this both for the baseline model and the lifting- and chaos-enhanced model. The difference between Fig. 7(a) and Fig. 7(b) is striking. For the baseline model, the weights corresponding to each class concentrate strongly in one element of the row (one coordinate in the m -dimensional space). This is understandable since the data we want to classify are perturbations of the canonical basis in \mathbb{R}^m and the distribution of the weights values across a row reflects this structure. As expected, the weight matrix is very efficient in identifying data from this particular class, assuming they are not heavily perturbed. On the other hand, for the lifting- and chaos-enhanced model, the weights corresponding to each row (class) fluctuate across the row (the coordinates in the m_{lift} -dimensional space) and thus can handle data which are more strongly perturbed. This result suggests an increased robustness to noise in the data by the lifting- and chaos-enhanced model.

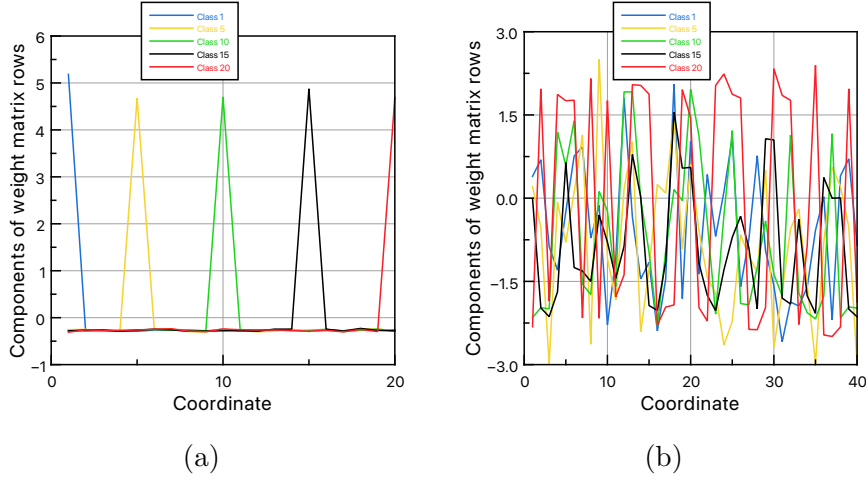


Figure 7: $m = 20$. Components of rows of the weight matrix (each row corresponds to a class) for the baseline model and the lifting- and chaos-enhanced model. To avoid clutter we have plotted only the weights for rows (classes) 1,5,10, 15 and 20. (a) Baseline model. (b) Lifting- and chaos-enhanced model. Note that the optimal m_{lift} determined during training is 40 and that is why there are 40 elements (coordinates) of the weight matrix in each row.

2.4 Robustness

We can provide a first insight into the increased robustness of the lifting- and chaos-enhanced model compared to the baseline and lifting-enhanced models by employing the proportion accuracy metric in (14) in addition to the alignment accuracy metric in (15). Fig. 8(a) shows the evolution of the testing proportion metric for the baseline, lifting-enhanced and lifting- and chaos-enhanced models (for 2 chaotic evolution temporal interval values). The proportion metric behaves similarly for all the models in terms of limiting value and rate of convergence.

However, the picture changes drastically when we include the alignment metric (as shown in Fig. 8(b)). Specifically, while for the lifting- and chaos-enhanced model, the alignment metric evolution tracks the proportion metric evolution, for the baseline and lifting-enhanced models the alignment metric evolution does *not* track the proportion metric evolution. In addition, the plateau reached by the alignment metric for the baseline and lifting-enhanced models is significantly below 1 (100%). This means that even though the baseline and lifting-enhanced models can predict 100% of

the correct labels for the test data (proportion metric equals 1), the corresponding confidence in the predictions is lacking. Moreover, if one stops training the baseline and lifting-enhanced models when the proportion metric reaches 1, which is after 130 epochs for the baseline model and 244 epochs for the lifting-enhanced model, respectively, the corresponding confidence in the predictions, given by the alignment metric is rather low, 36% for the baseline model and 77% for the lifting-enhanced model.

The confidence in the predictions of the baseline model suffers due to the lack of alignment of the predicted class probability vector with the correct label vectors. We attribute this fragility to the presence of noise in the data which makes the robust prediction of correct labels more difficult (recall the sharp concentration of the weight matrix rows on a single class as shown in Fig. 7(a)). The same argument applies to a lesser degree for the lifting-enhanced model which is more robust to noise, but still not as robust as the lifting- and chaos-enhanced model. A more detailed study to explain the agreement between the proportion and alignment metric for the lifting- and chaos-enhanced model will appear elsewhere.

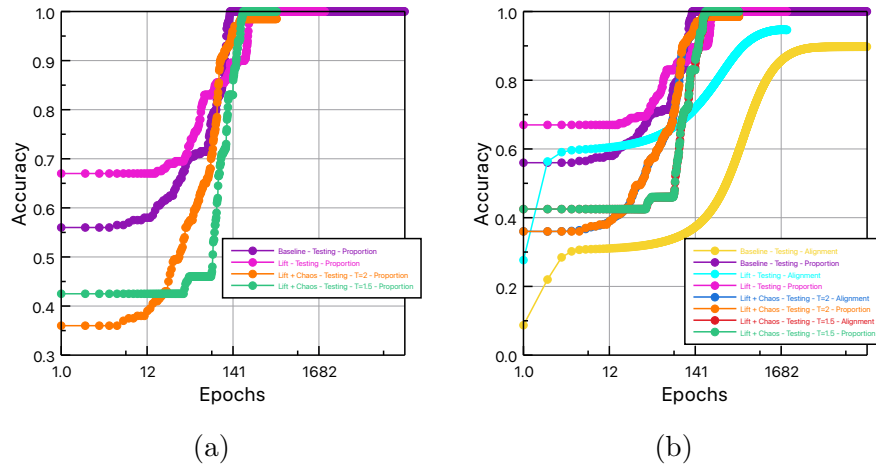


Figure 8: $m = 20$. (a) Proportion accuracy metric evolution with epochs for the baseline, lifting-enhanced and lifting- and chaos-enhanced models (for 2 different chaotic evolution temporal interval values). (b) Proportion and alignment accuracy metric evolution with epochs for the baseline, lifting-enhanced and lifting- and chaos-enhanced models (for 2 chaotic evolution temporal interval values).

2.5 Complexity

Finally, we comment on the computational complexity of the baseline model, the lifting-enhanced model and the lifting- and chaos-enhanced model. Table 1 presents the computational times in seconds for the three models for $m = 2, 10, 20$ (our calculations were run on an Apple M4 processor). We note that while for the baseline model we perform training for the dimension m for 20000 epochs, for the lifting-enhanced and the lifting- and chaos-enhanced models we train for a collection of lifting dimensions, in the range $(m + 6, 50)$. The computational times reflect the *total* time needed to train for all the allowed lifting dimensions. In addition, we have put an upper limit on the number of training epochs, 2000 epochs per lifting dimension value for the lifting-enhanced model and 500 for the lifting- and chaos-enhanced model. Upper limit means that the optimizer may not complete the allowed number of epochs. The reason this can happen is that the Adam optimizer was terminated if the loss value fell below 10^{-10} to avoid instability due to very small numbers.

For $m = 10, 20$, the lifting- and chaos-enhanced model requires more time to sweep across all the allowed lifting dimension cases and pick the optimal one than a single run of the baseline model. However, for the values of m reported in Table 1, the baseline model accuracy does not improve even if we let it train for time comparable to the one we need for the training of the lifting- and chaos-enhanced model. In addition, the testing accuracy of the lifting- and chaos-enhanced model is 100% for $m = 2, 10$ and 98.61% for $m = 20$ while the testing accuracy of the baseline model is 99.94% for $m = 2$, 95% for $m = 10$, and 90% for $m = 20$. Moreover, the robustness of the performance of the lifting- and chaos-enhanced model to the lifting dimension value, is a promising sign that one may not need to sweep a large number of lifting dimensions to find one which leads to high accuracy. With this in mind, the computational complexity of the lifting- and chaos-enhanced model becomes competitive to the baseline model while offering consistently superior accuracy.

m \ Model	Baseline	Lift	Lift + Chaos
2	0.28s	0.36s	0.25s
10	13s	110s	29s
20	151s	570s	170s

Table 1: Computing times for the 3 models (in seconds). The baseline model training runs for 20000 epochs, the lifting-enhanced model runs for up to 2000 epochs (per lifting dimension value) and the lifting- and chaos-enhanced for up to 500 epochs (per lifting dimension value). For the lifting-enhanced and the lifting- and chaos-enhanced models, the computing time is the total one required to sweep through the lifting dimensions $(m+6, 50)$ to determine the optimal one.

3 Discussion and future work

We have presented an approach to enhance classification accuracy that uses a two-stage approach where the input vector is first lifted to a higher dimension and then is evolved for a fixed temporal interval through a chaotic system. We observe that the lifting to higher dimensions, and especially the chaotic evolution, can accelerate significantly the training process and in addition increase the achieved accuracy compared to a baseline model. The rationale behind the combination of lifting to higher dimensions and chaotic evolution is to explore the available space in higher dimensions to pull apart the clusters of points corresponding to the various classes, but to do so in a controlled manner. Specifically, we can consider the evolution by a chaotic system as taking the cluster of points in the higher dimensional space corresponding to a class and blowing it up so that it occupies a larger volume. This, in turn, aids the classifier by making it easier to distinguish each class from the others. We have found that the lifting and chaotic evolution lead to much more uniform distribution of weight values within a row and also across rows (classes) compared to the baseline model. While these observations provide some insight into the improved performance of the proposed approach, a more thorough analysis based on the dynamics of training should be undertaken. Specifically, we need to understand how the lifting and chaotic evolution affect the gradient of the loss function.

The results presented here indicate that even though one can obtain dramatic increase in the classification performance without hyperparameter optimization, the benefits to be reaped can increase even more through a care-

ful analysis of the main elements of the proposed approach. These include the specific construction of the lifting to higher dimensions, the choice of the chaotic system to evolve the lifted vector as well as the temporal interval of the chaotic evolution. In addition, the use of more efficient stochastic optimizers than the standard Adam optimizer should also be considered. Also, we need to investigate further the seeming increase in robustness to noise in the data that is exhibited by the lifting- and chaos-enhanced model compared to the baseline model. Furthermore, it will be interesting to explore connections with physical reservoir computing approaches e.g., [22, 23, 24].

Finally, the results presented here are only proof-of-concept. A much more substantial test will be to see whether the proposed approach can improve the classification accuracy for challenging datasets e.g., standard benchmarks from image processing [25].

Acknowledgements

I would like to thank Shady Ahmed and Saad Qadeer for useful discussions and comments. This work is partially supported by the U.S. Department of Energy, Office of Science, Advanced Scientific Computing Research program under the "LEADS: LEarning-Accelerated Domain Science" project (Project No. 85462). Pacific Northwest National Laboratory is a multi-program national laboratory operated for the U.S. Department of Energy by Battelle Memorial Institute under Contract No. DE-AC05-76RL01830.

References

- [1] Sotiris B Kotsiantis, Ioannis D Zaharakis, and Panayiotis E Pintelas. Machine learning: a review of classification and combining techniques. *Artificial Intelligence Review*, 26(3):159–190, 2006.
- [2] Yann LeCun, Yoshua Bengio, and Geoffrey Hinton. Deep learning. *Nature*, 521(7553):436–444, 2015.
- [3] Stéphane Lathuilière, Pablo Mesejo, Xavier Alameda-Pineda, and Radu Horaud. A comprehensive analysis of deep regression. *IEEE transactions on pattern analysis and machine intelligence*, 42(9):2065–2081, 2019.

- [4] George Em Karniadakis, Ioannis G Kevrekidis, Lu Lu, Paris Perdikaris, Sifan Wang, and Liu Yang. Physics-informed machine learning. *Nature Reviews Physics*, 3(6):422–440, 2021.
- [5] Qi An, Saifur Rahman, Jingwen Zhou, and James Jin Kang. A comprehensive review on machine learning in healthcare industry: classification, restrictions, opportunities and challenges. *Sensors*, 23(9):4178, 2023.
- [6] Eduardo A Gerlein, Martin McGinnity, Ammar Belatreche, and Sonya Coleman. Evaluating machine learning classification for financial trading: An empirical approach. *Expert Systems with Applications*, 54:193–207, 2016.
- [7] Adi L Tarca, Vincent J Carey, Xue-wen Chen, Roberto Romero, and Sorin Drăghici. Machine learning and its applications to biology. *PLoS computational biology*, 3(6):e116, 2007.
- [8] Giuseppe Carleo, Ignacio Cirac, Kyle Cranmer, Laurent Daudet, Maria Schuld, Naftali Tishby, Leslie Vogt-Maranto, and Lenka Zdeborová. Machine learning and the physical sciences. *Reviews of Modern Physics*, 91(4):045002, 2019.
- [9] Kamal Choudhary, Brian DeCost, Chi Chen, Anubhav Jain, Francesca Tavazza, Ryan Cohn, Cheol Woo Park, Alok Choudhary, Ankit Agrawal, Simon JL Billinge, et al. Recent advances and applications of deep learning methods in materials science. *npj Computational Materials*, 8(1):59, 2022.
- [10] Peter J Bickel and Elizaveta Levina. Some theory for fisher’s linear discriminant function, naive bayes’, and some alternatives when there are many more variables than observations. *Bernoulli*, 10(6):989–1010, 2004.
- [11] Jianqing Fan and Yingying Fan. High dimensional classification using features annealed independence rules. *Annals of statistics*, 36(6):2605, 2008.
- [12] Bissan Ghaddar and Joe Naoum-Sawaya. High dimensional data classification and feature selection using support vector machines. *European Journal of Operational Research*, 265(3):993–1004, 2018.

- [13] Kento Nishi, Yi Ding, Alex Rich, and Tobias Hollerer. Augmentation strategies for learning with noisy labels. In *Proceedings of the IEEE/CVF conference on computer vision and pattern recognition*, pages 8022–8031, 2021.
- [14] Caimin An, Fabing Duan, François Chapeau-Blondeau, and Derek Abbott. Exploring the bayes-oriented noise injection approach in neural networks. *Physics Letters A*, page 130804, 2025.
- [15] Albert Kjølner Jacobsen, Johanna Marie Gegenfurtner, and Georgios Arvanitidis. Staying on the manifold: Geometry-aware noise injection. *arXiv preprint arXiv:2509.20201*, 2025.
- [16] Panos Stinis. Enforcing constraints for time series prediction in supervised, unsupervised and reinforcement learning. In *Proceedings of the AAAI 2020 Spring Symposium on Combining Artificial Intelligence and Machine Learning with Physical Sciences*. CEUR Workshop Proceedings, 2020.
- [17] Edward N Lorenz. Predictability: A problem partly solved. In *Proc. Seminar on predictability*, volume 1, pages 1–18. Reading, 1996.
- [18] Alireza Karimi and Mark R Paul. Extensive chaos in the lorenz-96 model. *Chaos: An interdisciplinary journal of nonlinear science*, 20(4), 2010.
- [19] Juan C Vallejo, Miguel AF Sanjuan, and Miguel AF Sanjuán. *Predictability of chaotic dynamics*. Springer, 2017.
- [20] Julien Brajard, Alberto Carrassi, Marc Bocquet, and Laurent Bertino. Combining data assimilation and machine learning to emulate a dynamical model from sparse and noisy observations: A case study with the lorenz 96 model. *Journal of computational science*, 44:101171, 2020.
- [21] Joel Lehman and Kenneth O Stanley. Abandoning objectives: Evolution through the search for novelty alone. *Evolutionary computation*, 19(2):189–223, 2011.
- [22] Chrisantha Fernando and Sampa Sojakka. Pattern recognition in a bucket. In *European conference on artificial life*, pages 588–597. Springer, 2003.

- [23] Gouhei Tanaka, Toshiyuki Yamane, Jean Benoit Héroux, Ryosho Nakane, Naoki Kanazawa, Seiji Takeda, Hidetoshi Numata, Daiju Nakano, and Akira Hirose. Recent advances in physical reservoir computing: A review. *Neural Networks*, 115:100–123, 2019.
- [24] Giulia Marcucci, Davide Pierangeli, and Claudio Conti. Theory of neuromorphic computing by waves: machine learning by rogue waves, dispersive shocks, and solitons. *Physical Review Letters*, 125(9):093901, 2020.
- [25] Li Deng. The mnist database of handwritten digit images for machine learning research [best of the web]. *IEEE signal processing magazine*, 29(6):141–142, 2012.